Reactions of Laser-Ablated Platinum and Palladium Atoms with Dioxygen. Matrix Infrared Spectra and Density Functional Calculations of Platinum Oxides and Complexes and Palladium Complexes

William D. Bare, Angelo Citra, George V. Chertihin, and Lester Andrews*

Department of Chemistry, University of Virginia, Charlottesville, Virginia 22901

Received: March 9, 1999; In Final Form: May 10, 1999

Platinum and palladium atoms produced by laser ablation were reacted with dioxygen diluted in argon during condensation at 10 K. Reaction products, including the $M(O_2)$ and $(O_2)M(O_2)$ complexes prepared with thermal metal atoms, and the platinum oxides PtO, OPtO, PtO_3, OOPtO, and $(O_2)PtO$, were analyzed by matrix infrared spectroscopy. Absorptions due to PdO and OPdO were not identified. Density functional theory (B3LYP) calculations were performed on product molecules, which were identified on the basis of isotopic frequency shifts and correlation with density functional calculations. The most interesting new molecule produced here, linear OPtO, can also be produced by photolysis of the cyclic $Pt(O_2)$ complex.

Introduction

The interaction of small gas molecules with bulk platinum and palladium is currently an area of intensive research. Much of this research has focused on the adsorption of these species (specifically O_2, N_2, and CO) on noble metal surfaces or on the catalytic reactions of such adsorbed species.[1−9] Also important are the reactions of dissolved gases on platinum and palladium surfaces, specifically the reduction of dissolved dioxygen on electrodes in fuel cells.[4,5] In the case of dioxygen, adsorption on platinum surfaces often leads to catalytic dissociation of the dioxygen molecule.[7−9]

Matrix isolation infrared spectra have been reported for the dioxygen complexes of platinum and palladium prepared from thermal evaporation of the metal.[10] Emission spectra have given the frequency and dipole moment of PtO in the gas phase.[11−14] Electron energy loss spectroscopy has been used to study the adsorption and dissociation of O_2 on platinum surfaces, and a strong 860 cm^{-1} signal has been attributed to an absorbed species with an O—O single bond.[1] Raman spectroscopy has been used to investigate reactions of NO and CO on platinum and on palladium.[15] The current paper reports the reactions of laser-ablated platinum and palladium atoms with dioxygen, forming the dioxygen complexes and the platinum oxides PtO, OPtO, PtO_3, OOPtO, and $(O_2)PtO$.

Experimental Section

The technique and apparatus for laser ablation and matrix isolation FTIR spectroscopy have been described previously.[16] Platinum (from crucible) and palladium (Johnson-Mathey) targets were mounted on a rotating (1 rpm) stainless steel rod. The pulsed (10 Hz, 20−40 mJ/pulse) Nd:YAG 1064 nm fundamental was focused on the target through a hole in the 10 K CsI window. Dilute (0.2%−1.0%) or more concentrated (2%−5%) oxygen in argon was co-deposited with the ablated metal atoms onto the cryogenic window for 1−2 h. Combinations of isotopically enriched oxygen ($^{18}O_2$, "mixed" = $^{16}O_2/^{18}O_2$, and "scrambled" = $^{16}O_2/^{16}O^{18}O/^{18}O_2$) samples were used in subsequent experiments. Spectra were recorded on a Nicolet 750 FTIR spectrophotometer, using 0.5 cm^{-1} resolution. Matrices were subjected to broadband photolysis by a medium-pressure mercury arc lamp (Philips, 175 W, with globe removed) and to several annealing−recooling cycles, with spectra recorded after each event.

Calculations

Density functional theory calculations were performed on expected monoxide, dioxide, and trioxide products using the Gaussian 94 program,[17] the B3LYP functional,[18] with the D95* basis set for oxygen[19] and the LanL2DZ basis set and pseudopotentials for palladium and platinum.[20] Calculated geometries and vibrational frequencies for these molecules are given in Tables 1−3.

Since PtO is the only molecule observed here that has also been characterized in the gas phase[11−14] and by recent calculations using density functional theory including relativistic effects,[21,22] we use PtO as a test case. Although the $^1\Sigma$ ground state was first proposed,[11] more recent experimental data agree on the $^3\Sigma^-$ ground state.[12−14] Our density functional calculations, using both B3LYP and BP86 functionals with pseudopotentials for Pt, find $^3\Sigma^-$ substantially lower (B3LYP, 29.1 kcal/mol; BP86, 27.9 kcal/mol) than $^1\Sigma^+$ and the calculated frequency for the $^3\Sigma^-$ state (B3LYP, 865 cm^{-1}; BP86, 861 cm^{-1}) in excellent agreement with the 851 cm^{-1} gas-phase harmonic frequency.[11] In addition, the earlier frequency calculations including relativistic effects for the $^3\Sigma^-$ state, $\pi^3\sigma^1$, "harmonic" frequency (852, 801 cm^{-1})[21,22] are near the present B3LYP/ECP value and the experimental harmonic frequency (851 cm^{-1}).[11] Furthermore, the bond length and dipole moment calculated by B3LYP (1.749 Å, 2.66 D) are in very good agreement with experiment (1.727 Å, 2.77 D).[14] Hence, the present simple B3LYP and pseudopotentials with an approximate treatment of relativistic effects and the more sophisticated density functional theory with relativistic corrections[21,22] predict frequencies for $^3\Sigma^-$ PtO that are in reasonable agreement with the gas-phase observation[11,12] and the matrix spectrum of PtO that follows. We will use this simple B3LYP/ECP calculation as an approximation for larger platinum oxides to model the ground-state vibrational potentials and thus to help assign products in the matrix infrared spectrum.

10.1021/jp990823e CCC: $18.00
Published on Web 06/24/1999

TABLE 1: Density Functional (B3LYP) Calculated Energies, Geometries, and Frequencies for PdO and PdO_2 Isomers

molecule[a]	energy vs OPdO (kcal/mol)	bond length (Å)	bond angle (deg)	frequency (cm^{-1}), intensity (km/mol), and symmetry of vibration
PdO, $^3\Sigma^-$		1.865		563, 7, σ
OPdO, $^5A_1$	0.0	1.886 (Pd−O)	168.1 (OPdO)	120, 19, a_1; 453, 48, b_2; 597, 0.4, a_1
OPdO, $^3\Sigma_g^+$	+17.1	1.803 (Pd−O)	180.0 (OPdO)	120, 86, π_u; 465, 0.2, σ_u; 730, 0, σ_g
Pd(O_2), $^1A_1$	+28.4	2.047 (Pd−O)	38.0 (OPdO)	253, 11, b_2; 382, 3, a_1; 1173, 66, a_1
		1.332 (O−O)		
PdOO, $^3A''$	+48.7	2.063 (Pd−O)	111.2 (PdOO)	147, 0.3, a′; 334, 5, a′; 1353, 348, a″
		1.267 (O−O)		

[a] $\langle S^2\rangle$ values: $^3\Sigma^-$ PdO (2.001), $^3\Sigma_g^+$ OPdO (2.006), $^3A''$ PdOO (2.000).

TABLE 2: Density Functional (B3LYP) Calculated Energies, Geometries, and Frequencies for PtO and PtO_2 Isomers

molecule[a]	energy vs OPtO (kcal/mol)	bond length (Å)	bond angle (deg)	frequency (cm^{-1}), intensity (km/mol), and symmetry of vibration
PtO,[b] $3\Sigma^-$	0.0	1.749		865, 30, σ
PtO, $^1\Sigma$	+29.1	1.742		881, 46, σ
OPtO,[b–d] $^1\Sigma_g^+$	0.0	1.707 (Pt−O)	180.0 (OPtO)	135.7, 4, π_u; 996.3, 0, σ_g; 1052.7, 136, σ_u
OPtO, $^3A_2$	+23.4	1.760 (Pt−O)	136.3 (OPtO)	180, 5, a_1; 849, 33, b_1; 856, 3, a_1
Pt(O_2), $^1A_1$	+46.2	1.979 (Pt−O)	40.9 (OPtO)	450, 13, b_2; 471, 0.04, a_1; 1065, 19, a_1
		1.383 (O−O)		
PtOO, $^3A''$	+34.7	1.924 (Pt−O)	112.8 (PtOO)	195, 0.5, a′; 532, 4, a′; 1298, 263, a′
		1.274 (O−O)		

[a] $\langle S^2\rangle$ values: $^3\Sigma^-$ PtO (2.000), $^3A_2$ OPtO (2.009), $^3A''$ PtOO (2.000). [b] Mulliken charges: Pt (+0.35), O (−0.35), ($^1\Sigma_g^+$) O (−0.46), Pt (+0.92), O (−0.46). [c] Calculated stretching frequencies. For $^{16}OPt^{18}O$: 1037.5 (115 km/mol), σ, 957.1 (15 km/mol), σ. For $^{18}OPt^{18}O$: 1001.1 (123), σ_u, 939.2 (0), σ_g. [d] The BP86 calculation for OPtO gave 1.721 Å, linear, 152 cm^{-1} (2 km/mol), 951 cm^{-1} (0 km/mol), 1008 cm^{-1} (104 km/mol), for comparison.

TABLE 3: Density Functional (B3LYP) Calculated Energies, Geometries, and Frequencies for PtO_3 Isomers and (O_2)Pt(O_2) Structures

molecule[a]	relative energy (kcal/mol)	bond length (Å)	bond angle (deg)	frequency (cm^{-1}), intensity (km/mol), and symmetry of vibration
(O_2)PtO, $^3B_2$	0.0	1.748 (Pt−O)	161.5 (OPtO)	136, 0.3, b_2; 204, 1, b_1; 420, 4, a_1
		2.048 (Pt−O)	37.0 (OPtO)	492, 1, b_2; 868, 35, a_1; 1265, 101, a_1
		1.300 (O−O)		
PtO_3,[b] $^3A'_1$	+4.9	1.757 (Pt−O)	120.0 (OPtO)	251, 0.2 × 2, e; 255, 5, a_2''; 839, 20 × 2, e; 885, 0.0, a_1'
OOPtO, $^5A'$	+11.9	1.793 (Pt−O)	177.5 (OPtO)	88, 10, a′; 161, 1, a′; 210, 12, a′
		2.092 (Pt−OO)	102.9 (PtOO)	392, 6, a′; 796.3, 2, a′; 1324.1, 480, a′
		1.264 (O−O)		
(O_2)Pt(O_2), ^1A_g (D_{2h})	0.0	1.985 (Pt−O)	39.4 (OPtO)	403, 0, a_u; 472, 0, a_g; 490, 9, b_{1u}
		1.338 (O−O)		588, 1, b_{2u}; 1105, 529, b_{1u}; 1174, 0, a_g
(O_2)Pt(O_2), $^1A_1$ (D_{2d})	+1.7	1.707 (Pt−O)	41.1 (OPtO)	253, 0, b_1; 342, 6 × 2, e; 443, 0, a_1
		1.380 (O−O)		509, 0, b_2; 1079, 0, a_1; 1112, 6, b_2

[a] $\langle S^2\rangle$ values: $^3B_2$ (O_2)PtO (2.000), $^3A_1$ PtO_3 (2.000), $^5A'$ OOPtO (6.000). [b] Mulliken charges: Pt (+1.27), O (−0.423).

The most important new molecule reported here, OPtO, is calculated to have the linear $^1\Sigma_g^+$ ground state by both B3LYP and BP86 functionals and frequencies in good agreement with the matrix observation.

Results

Laser-ablated palladium and platinum experiments with dioxygen will be described in turn.

Pd. Reactions of laser-ablated palladium with dioxygen produced strong absorptions due to dioxygen complexes. Bands were observed at 1110.0 and 1023.4 cm^{-1}, which were shifted to 1047.6 and 966.0 cm^{-1} with $^{18}O_2$. These two bands produced triplet and doublet patterns, respectively, when the mixed $^{16}O_2$ + $^{18}O_2$ sample was used. These observations are in agreement with a thermal Pd investigation where these bands were assigned to (O_2)Pd(O_2) and Pd(O_2), respectively.[10] In addition, photosensitive bands observed in this region at 1118.6, 1039.6, and 953.8 cm^{-1} for O_4^+, ozone, and O_4^- are characteristic of laser-ablated metal experiments with O_2.[23−26] The 1023.4 cm^{-1} band *did not* decrease on photolysis, in contrast to the analogous Pt species. An experiment with N_2O in argon gave no oxide products. Finally, experiments were done with 1% O_2 in nitrogen and a strong new 997.7 cm^{-1} band was observed, which shifted to 942.4 cm^{-1} with $^{18}O_2$.

More aggressive procedures were employed to produce new palladium products, including the use of concentrated (2%−5%) O_2 samples in argon and of high-intensity mercury arc photolysis during deposition. Neither of these techniques produced new bands.

Pt. Infrared spectra of reaction products of laser-ablated platinum with dioxygen are shown in Figures 1 and 2, and the observed infrared absorptions are listed in Table 4. A strong, sharp band was observed following sample deposition at 953.3 cm^{-1}, along with a weaker satellite at 961.8 cm^{-1}. Annealing to 25 and 30 K decreased the upper band, and further annealing to 35 and 40 K decreased the lower band; the 961.8 cm^{-1} band showed significant (+100%) growth on photolysis of the matrix (Figure 1c). Substitution with $^{18}O_2$ shifted these bands to 907.0 and 914.9 cm^{-1}. The experiment using mixed isotopic oxygen ($^{16}O_2$ + $^{18}O_2$) produced primarily the two pure isotopic bands discussed above; however, two weak intermediate bands were also observed to be split at 939.3, 938.0 cm^{-1} and at 947.3 cm^{-1}. This experiment produced only pure isotopic bands as a result of photolysis, while both pure and intermediate isotopic bands

TABLE 4: Observed Infrared Absorptions (cm^{-1}) for Reaction Products of Laser-Ablated Platinum and Palladium Atoms with Various Isotopic Mixtures of Dioxygen, Isolated in Solid Argon at 10 K

$^{16}O_2$	$^{18}O_2$	$^{16}O_2 + {}^{18}O_2$	$^{16}O_2 + {}^{16}O^{18}O_2 + {}^{18}O_2$	ratio	assignment
1402.1	1323.6	1402.1, 1372.4, 1354.7, 1323.6	1402.1, 1372.4, 1354.7, 1323.6	1.0593	OOPtO
1174.2	1108.6	1174.2, 1108.6	1174.2, 1142.0, 1108.6	1.0592	$(O_2)PtO$
1110.1	1047.6			1.0596	$(O_2)Pd(O_2)$
1023.0	966.0			1.0590	$Pd(O_2)$
1051.3	992.6			1.0591	$(O_2)Pt(O_2)$
961.8	914.9	961.8, 914.9	961.8, 947.3, 914.9; 870.1, ν_1	1.0512	OPtO ν_3 site 1
953.3	907.0	953.3, 914.9	953.3, 939.3, 907.0, ?	1.0510	OPtO ν_3 site 2
928.0	876.6	928.0, 876.6	928.0, 903.0, 876.6	1.0586	$Pt(O_2)$ ν_3
875.8	831.1			1.0538	?
868.0	823.1	868.0, 847.2, 823.1	868.0, 847.3, 823.1	1.0545	?
833.4	791.5	833.4, 809.1, ?, ?	833.4, 809.1, 803.9, 791.5 ?	1.0530	(PtO_3)
828.0	784.4	828.0, 784.4	828.0, 784.4	1.0555	PtO site 1
823.0	779.8	823.0, 779.8	823.0, 779.8	1.0554	PtO site 2
550.9	520.8	550.9, 520.8	550.9, 538.5, 520.8	1.0578	$((PtO)_2)$

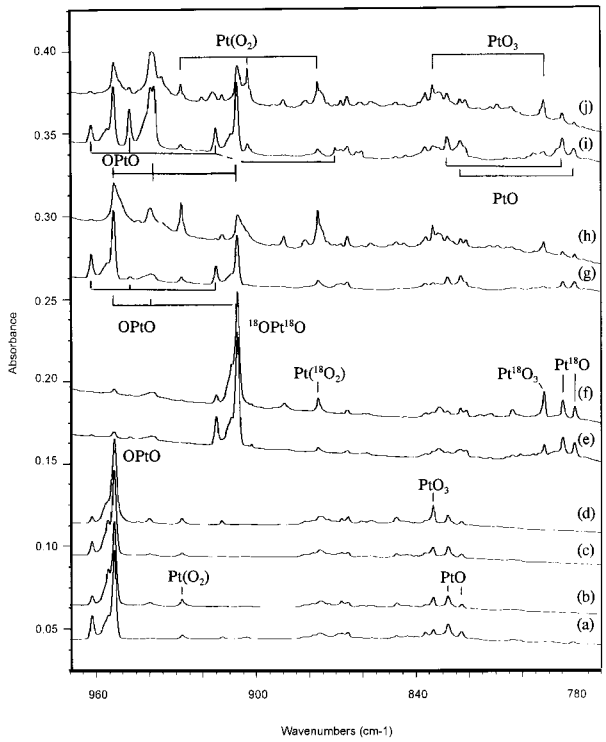

Figure 1. Infrared spectra in the 970−770 cm^{-1} region for samples prepared by co-condensation of laser-ablated Pt atoms with O_2 in argon: (a) 2% $^{16}O_2$ after co-deposition; (b) after annealing to 30 K; (c) after broadband photolysis for 30 min; (d) after annealing to 35 K; (e) 1% $^{18}O_2$ after co-deposition; (f) after annealing to 35 K; (g) 0.75% $^{16}O_2$ + 0.75% $^{18}O_2$ after co-deposition; (h) after annealing to 35 K; (i) 0.25% $^{16}O_2$ + 0.5% $^{16}O^{18}O$ + 0.25% $^{18}O_2$ after deposition; (j) after annealing to 35 K.

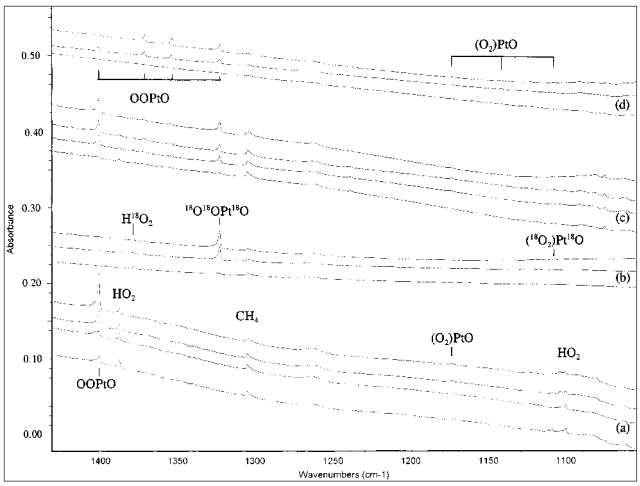

Figure 2. Infrared spectra in the 1430−1060 cm^{-1} region for samples prepared by co-condensation of laser-ablated Pt atoms with O_2 in argon: (a) 2% $^{16}O_2$ after co-deposition; (b) 1% $^{18}O_2$ after co-deposition; (c) 0.75% $^{16}O_2$ + 0.75% $^{18}O_2$ after co-deposition; (d) 0.25% $^{16}O_2$ + 0.5% $^{16}O^{18}O$ + 0.25% $^{18}O_2$ after deposition. The additional spectra in each set were recorded following successive annealings to 25, 30, and 35 K (three scans) or to 30 and 35 K (two scans). Photolysis after (a) reduced the 1402.1 cm^{-1} band.

increased slightly as a result of annealing. In the experiment using scrambled oxygen ($^{16}O_2/^{16}O^{18}O/^{18}O_2$) the upper band was produced in a 1:2:1 ratio, but the lower band intermediate component appeared split (Figure 1(i)). A weaker band at 870.1 cm^{-1} (10% as intense as the 947.3 cm^{-1} band) tracked with the 947.3 cm^{-1} band on annealing−photolysis cycles in two scrambled isotopic experiments.

A weak band was observed following deposition at 928.0 cm^{-1}. This band grew markedly (+100%) following annealing and was strongly attenuated (−50%) by photolysis (Figure 1c). Substitution with $^{18}O_2$ shifted this band to 876.6 cm^{-1}. A new intermediate band was observed following deposition at 903.0 cm^{-1} in the experiment using isotopically scrambled oxygen but not with the simple isotopic mixture. This band is due to cyclic $Pt(O_2)$ as assigned previously.[10]

A sharp band at 833.4 cm^{-1} present following deposition of the matrix grew substantially following annealing to higher temperatures (25, 30, and 35 K). This band was shifted to 791.5 cm^{-1} with $^{18}O_2$. Any intermediate bands formed in the isotopically mixed and scrambled experiments are much weaker; possible candidates at 809.1 and 803.9 cm^{-1} tracked on annealing with the 833.4 and 791.5 cm^{-1} bands, but another component could be masked near 820 cm^{-1}.

A pair of bands at 828.0 and 823.0 cm^{-1} was observed following deposition. These bands showed a slight increase following annealing and were not appreciably affected by photolysis. Isotopic substitution shifted these bands to 784.4 and 780.0 cm^{-1} with no new bands appearing in the mixed or scrambled isotopic experiments.

A weak, sharp band at 1051.3 cm^{-1} following deposition increased on annealing and also on photolysis. Substitution with $^{18}O_2$ shifted this band to 992.6 cm^{-1}. The presence of bands due to ozone made it difficult to conclusively identify intermediate components in the experiments employing mixed and scrambled isotopic oxygen.

A weak, broad band was observed at 550.9 cm^{-1}. This band grew slightly on annealing and was attenuated by photolysis. Substitution with $^{18}O_2$ shifted the band to 520.8 cm^{-1}. No isotopic intermediates were observed in the mixed $^{16}O_2$ + $^{18}O_2$

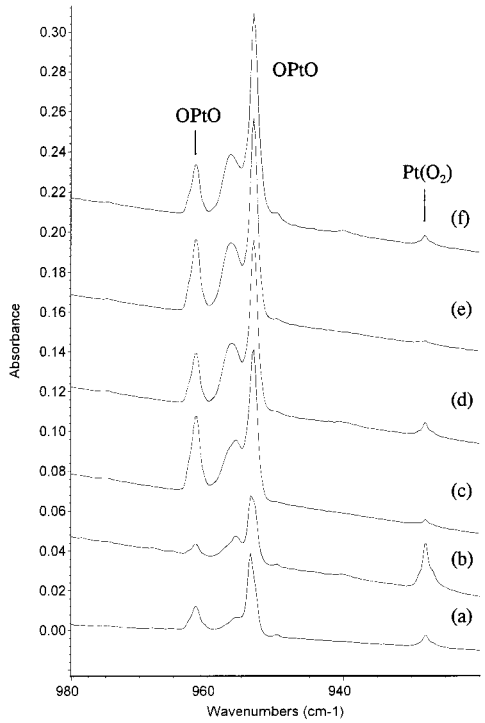

Figure 3. Infrared spectra in the 980−920 cm^{-1} region for laser-ablated Pt atoms co-deposited with 1% O_2 in argon: (a) sample deposited at 10 K for 1.5 h; (b) after annealing to 25 K; (c) after broadband photolysis for 30 min; (d) after annealing to 30 K; (e) after broadband photolysis for another 30 min; (f) after final annealing to 35 K.

sample, but a 1:2:1 isotopic triplet pattern was observed when in the scrambled isotopic experiment with an intermediate component at 538.5 cm^{-1}.

In the upper spectral region, weak bands increased on annealing to 25, 30, and 35 K at 1402.1 cm^{-1} and at 1174.2 cm^{-1} in addition to weak HO_2 and CH_4 impurity absorptions.[27] The upper band shifted to 1323.6 cm^{-1} with $^{18}O_2$ and gave weak mixed isotopic components with isotopically mixed oxygen but exhibited a 1:1:1:1 quartet with isotopically scrambled oxygen. Substitution with $^{18}O_2$ shifted the lower band to 1108.6 cm^{-1}; no new intermediate bands were observed in the mixed sample, while the scrambled sample produced a 1:2:1 triplet, with an intermediate component at 1142.0 cm^{-1}.

Photolysis behavior was examined in a more dilute O_2 experiment, and the spectra are shown in Figure 3. Note that first annealing to 25 K markedly increases the 928.0 cm^{-1} band and slightly decreases the 961.8 and 953.3 cm^{-1} bands. Broadband photolysis *markedly increases* both 961.8 and 953.3 cm^{-1} bands and *decreases* the 928.0 cm^{-1} band. Further annealing to 30 K restores some of the 928.0 cm^{-1} band, but more photolysis again reduces the 928.0 cm^{-1} band and increases the 961.8 and 953.3 cm^{-1} absorptions. A very weak 1053.1 cm^{-1} band increases on annealing and is not affected by photolysis.

Discussion

The product molecules will be identified from isotopic substitution and comparison to density functional calculations.

$Pd(O_2)$. The band observed at 1023.4 cm^{-1} and its $^{18}O_2$ counterpart at 966.7 cm^{-1} are in agreement with the previous report by Huber and co-workers for the cyclic $Pd(O_2)$ complex.[10] These bands *did not* decrease on photolysis in contrast to $Pt(O_2)$ discussed below. The nitrogen matrix counterpart was observed here at 997.7 cm^{-1}. Our B3LYP calculation predicts this strong band at 1173.3 cm^{-1}, which must be scaled by 0.87 to match the observed frequency. This scale factor is smaller than values for the B3LYP functional and basis set for selected transition metal compounds,[28] which shows that higher level calculations are needed for Pd/O_2 systems. Finally, the band that appears at 1110.0 cm^{-1} on annealing is in agreement with the earlier assignment to the $(O_2)Pd(O_2)$ complex.[10]

PdO. The B3LYP calculations reported here predict a vibrational frequency near 560 cm^{-1} for the PdO molecule, which is compatible with the 608 cm^{-1} value calculated earlier for $^3\Sigma^-$ ground-state PdO.[22] Our calculations suggest that the $^1\Sigma^+$ state is 25.0 kcal/mol higher. We have found no gas-phase spectrum of PdO.[29] No band was observed that showed the necessary isotopic frequency shift for assignment to PdO in these experiments. Our B3LYP calculations indicate that reaction 1 is strongly endothermic. This high endothermicity is probably a result of the very stable (d^{10}) electronic configuration of the ground-state palladium atom, which contrasts with the (s^2d^8) and (s^1d^9) configurations of nickel and platinum, respectively, in the same group.

$$Pd + O_2 \rightarrow PdO + O \qquad (\Delta E = +64.2 \text{ kcal/mol}) \quad (1)$$

OPdO. No bands were observed that could be attributed to the OPdO molecule, on the basis of isotopic shifts, even following illumination with a high-intensity mercury arc lamp. Such photolysis produced OPtO from $Pt(O_2)$ in the analogous Pt/O_2 experiments. Our B3LYP calculations predict OPdO to have $^5A_1$ ground state in contrast to OPtO and ONiO, which have $^1\Sigma_g^+$ ground states. For OPdO, the singlet state is bent (150°) and is 16.1 kcal/mol higher than the ground state. Although one expects the formation of OPdO to have a high activation energy barrier, the DFT calculations performed here indicate that reaction 2 is also substantially endothermic, which helps account for nonobservation of the OPdO species.

$$Pd + O_2 \rightarrow OPdO \qquad (\Delta E = +10.4 \text{ kcal/mol}) \quad (2)$$

PtO. Absorption bands observed at 828.0 and 823.0 cm^{-1} are assigned as two sites of PtO in solid argon. These absorptions exhibit 16/18 isotopic frequency ratios of 1.0555 and 1.0554, just below the harmonic diatomic ratio of 1.0557, and showed no evidence of any intermediate isotopic component in the mixed or scrambled experiments. This observed frequency is in agreement with the 865 cm^{-1} prediction from B3LYP calculations and earlier calculations[21,22] for the $^3\Sigma^-$ ground state and the 841.1 cm^{-1} fundamental deduced from the emission spectrum.[11,12] The scale factor 0.97 required to fit the gas-phase PtO frequency is appropriate for this system.[28] In fact the observation of PtO at 828.0 cm^{-1} in solid argon, in very good agreement with calculated $^3\Sigma^-$ state frequencies, provides corroboration for the identification of $^3\Sigma^-$ as the ground state.

$Pt(O_2)$. The absorption at 928.0 cm^{-1} is assigned to the symmetric O−O stretching mode of the cyclic $Pt(O_2)$ complex, in agreement with Huber et al.[10] This band showed no intermediate component in the mixed isotopic experiment and a 1:2:1 triplet in the scrambled experiment, as expected for a molecule with two equivalent oxygen atoms. Note that unlike the OPtO species, discussed below, the 1:2:1 triplet pattern is symmetric, with the intermediate isotopic component very near the average of the pure isotopic bands. This indicates that the Pt−O_2 symmetric stretch for this molecule is much lower and is consistent with the B3LYP calculated frequencies. Although our B3LYP calculations suggest that PtOO is lower energy than $Pt(O_2)$, the observed spectrum is not appropriate in terms of

region or isotopic splittings for PtOO. The B3LYP calculation requires a 0.87 scale factor to fit the 928.0 cm^{-1} band, as did the analogous band for the $^1A_1$ state of PdO_2. This is lower than the PtO scale factor and other scale factors for the B3LYP functional,[28] which suggests that a higher level of theory is required for a proper description of $Pt(O_2)$.

$(O_2)Pt(O_2)$. The 1051.3 cm^{-1} band that increased on annealing and shifted to 992.6 cm^{-1} with $^{18}O_2$ is in agreement with the previous observations and assignment of these bands to the $(O_2)Pt(O_2)$ complex.[10] Our DFT calculations find stable D_{2d} and D_{2h} structures for $(O_2)Pt(O_2)$ with 1112.4 and 1105.5 cm^{-1} antisymmetric O−O stretching modes, and the D_{2h} form has a much stronger calculated infrared band and is 1.7 kcal/mol lower, which is little basis for choice at this level of theory. The scale factor (0.95) for both structures is reasonable. However, calculations predict the symmetric O−O stretching mode to be *higher* than the antisymmetric O−O stretching mode for the D_{2h} molecule but *the reverse order* for the D_{2d} structure. This is critical for the $(^{16}O^{16}O)Pt(^{18}O^{18}O)$ isotopic molecule, since these modes can interact and the observed antisymmetric mode for this mixed isotopic molecule will be displaced *blue* for the D_{2d} structure and *red* for the D_{2h} structure. The thermal Pt spectra for $^{16}O_2 + {}^{18}O_2$ (1050.0, 1004.0, 991.4 cm^{-1}) show 46.0 and 12.6 cm^{-1} band separations, and the calculated (harmonic) D_{2h} isotopic band separations are 44.7, 18.2 cm^{-1}, whereas the calculated D_{2d} isotopic band separations are 12.6 and 50.6 cm^{-1}, respectively. Clearly, the calculated mixed isotopic band position gives a strong preference for the lower energy D_{2h} structure. Furthermore, the infrared absorptions for all intermediate isotopic molecules[10] are displaced lower owing to interaction with the higher symmetric O−O stretching mode. In addition, the cis−trans splitting in the $(^{16}O^{18}O)Pt(^{16}O^{18}O)$ isotopic molecule is calculated to be 0.2 cm^{-1}, much too small to resolve in these experiments. Hence, these DFT calculations suggest that the $(O_2)Pt(O_2)$ complex in fact has the D_{2h} structure rather than the D_{2d} form first proposed.[10]

The analogous conclusion was reached about the $(O_2)Ni(O_2)$ molecule from DFT calculations using the BP86 functional.[30] Here, we have repeated the $(O_2)Ni(O_2)$ calculation using the B3LYP functional. We find a stable D_{2h} structure for $(O_2)Ni(O_2)$, and the D_{2d} form is much higher (44 kcal/mol). We again conclude that $(O_2)Ni(O_2)$ is a planar complex. The mixed isotopic spectra for $(O_2)Pd(O_2)$ exhibit the same red displacements,[10] and this complex is also probably planar.

OPtO. The strong, sharp absorptions at 961.8 and 953.3 cm^{-1} are assigned to two sites of the antisymmetric stretching mode of the new linear OPtO molecule. In the scrambled isotopic experiment an intermediate band was observed giving a triplet with a 1:2:1 intensity ratio for the upper 961.8, 947.3, 914.9 cm^{-1} band, indicating the presence of two equivalent oxygen atoms in this molecule; the weaker 870.1 cm^{-1} band tracks with the 947.3 cm^{-1} band and is due to the "symmetric" stretching mode of $^{16}OPt^{18}O$. The intermediate component was site-split for the lower band presumably because of a matrix interaction with one end of the molecule. The asymmetry of the triplet pattern, with the central band approximately 9 cm^{-1} higher than the average of the pure isotopic bands, is evidence of interaction with a nearby vibrational mode in this molecule that is lower, and the weak 870.1 cm^{-1} band is assigned accordingly. This is in agreement with the B3LYP calculations, which not only predict the ν_3 mode of $^{16}OPt^{16}O$ at 1052.7 cm^{-1} (scale factor 0.91 to fit observed matrix band) but also find a ν_1 mode approximately 56 cm^{-1} lower. Furthermore, the B3LYP calculation predicts the "symmetric" stretching mode of $^{16}OPt^{18}O$ to be some 80 cm^{-1} lower and with 13% of the intensity of the "antisymmetric" mode. This is in excellent agreement with the observed spectrum and confirms the present observation of linear OPtO.

The 1.0512 and 1.0510 oxygen 16/18 isotopic frequency ratios are much lower than the ratio observed for PtO, as is expected for the antisymmetric stretch of an O−M−O molecule with a large obtuse angle. The theoretical harmonic ratio for the linear species is 1.0514. Accordingly, the OPtO molecule is linear like ONiO observed previously.[30] Finally, the calculated Mulliken charges[17] on O (−0.46), Pt (+0.92), O (−0.46) show that platinum is more highly oxidized in OPtO than in PtO.

The lack of a strong intermediate isotopic band in the $^{16}O_2 + {}^{18}O_2$ mixed isotopic experiment provides evidence that OPtO is predominantly formed by reaction with a single oxygen molecule. It is clear from the failure of Huber and co-workers to observe OPtO that thermal platinum atoms do not insert into dioxygen, which was also the case for nickel.[10,31] The B3LYP calculations performed here indicate that the insertion reaction by ground-state platinum atoms, as in reaction 3, is significantly exothermic.

$$Pt + O_2 \xrightarrow{E_a} [OPtO]^* \xrightarrow{\text{relax}} OPtO \qquad (\Delta E = -54.8 \text{ kcal/mol}) \quad (3)$$

It follows that although the insertion reaction is exothermic, the reaction has a high activation barrier, probably associated with cleavage of the O−O bond. In the absence of photolysis, the less exothermic reaction 4 forming $Pt(O_2)$ occurs preferentially because of its lower, if any, energy of activation.

$$Pt + O_2 \xrightarrow{\text{anneal}} Pt(O_2) \qquad (\Delta E = -8.6 \text{ kcal/mol}) \quad (4)$$

Laser ablation provides platinum atoms with sufficient excess energy to activate the insertion reaction; this excess energy may be translational or metastable electronic.

Also important in understanding the formation of this molecule is the observation that bands due to OPtO consistently increase following photolysis, while those due to $Pt(O_2)$ decrease. Taken together, these observations are strong evidence that an important mechanistic pathway for the formation of OPtO is photolysis of $Pt(O_2)$, as in reaction 5, which B3LYP calculations predict to be strongly exothermic. Photolysis by the laser plume may account for the formation of OPtO by reaction 5 during deposition. It should be noted that $Ni(O_2)$ also photoisomerizes to give linear ONiO in solid argon.[31]

$$Pt(O_2) \xrightarrow{\text{photolysis}} OPtO \qquad (\Delta E = -46.2 \text{ kcal/mol}) \quad (5)$$

In the $^{16}O_2 + {}^{18}O_2$ experiments, a very weak intermediate isotopic $^{16}OPt^{18}O$ band was observed following deposition, although no isotopic intermediates were seen for the $Pt(O_2)$ molecule. This indicates that a second reaction pathway must also be available for the formation of OPtO. In this experiment, the band due to the intermediate grew slightly, relative to the pure isotopic bands, during the course of several annealing cycles, growing from 5% of the size of the $^{16}OPt^{16}O$ band initially to approximately 15% of the intensity of the $^{16}OPt^{16}O$ band at the end of several annealing cycles. No growth of the isotopic intermediate band was observed following photolysis. The growth of the intermediate band is evidence that the OPtO molecule is also formed (although to a much lesser extent) during annealing, by an addition reaction involving two separate

oxygen-containing species, probably the addition of free oxygen atoms to PtO, as in reaction 6:

$$O + PtO \rightarrow OPtO \quad (\Delta E = -87.4 \text{ kcal/mol}) \qquad (6)$$

For this mechanism to contribute to the formation of OPtO, the intermediate band must increase at twice the rate of the pure isotopic bands during annealing, as is observed. Furthermore, absorptions due to ozone in all experiments provide evidence of the existence of free oxygen atoms in the matrix, and the slight growth of ozone bands attests to the diffusion of oxygen atoms during annealing.

It is interesting to contrast the stable $(O_2)Pt(O_2)$ complex formed on annealing,

$$O_2 + Pt(O_2) \rightarrow (O_2)Pt(O_2) \qquad (\Delta E = -59.3 \text{ kcal/mol}) \quad (7)$$

with a possible dioxygen complex of platinum dioxide, as the latter analogue $(O_2)IrO_2$ is formed instead of $(O_2)Ir(O_2)$ in the iridium and oxygen experiments.[32] However, the linear singlet OPtO forms only a very weak complex (4.061 Å separation) with O_2 (+13.1 kcal/mol above the $(O_2)Pt(O_2)$ complex), and the same applies to bent triplet OPtO, which is 23.4 kcal/mol higher than the singlet and still does not bind O_2.

PtO_3. The weak 833.4 cm^{-1} band increased substantially on annealing and was not affected by photolysis. The $^{18}O_2$ shift to 791.5 cm^{-1} defines a 16/18 ratio (1.0530) that is intermediate between diatomic PtO and linear OPtO. Both mixed isotopic experiments revealed *possible weaker* intermediate components (in contrast to OPtO), which suggests the doubly degenerate mode of a trigonal species.[33] Furthermore, the 16/18 ratio estimates an upper limit of 130° to the valence angle for this antisymmetric O−Pt−O stretching mode, and B3LYP calculations predict ν_3 of the D_{3h} PtO_3 molecule at 839.4 cm^{-1} just (almost 1%) above the observed value. These results support tentative assignment of the 833.4 cm^{-1} band to PtO_3. Without a definitive observation of the weaker intermediate components, we cannot be more specific about structure. This trioxide is formed by the addition of a third O atom to either OPtO or $Pt(O_2)$. The PtO_3 band yield increases relative to PtO with increasing O_2 concentration in these experiments.

$$O + OPtO \text{ or } Pt(O_2) \rightarrow PtO_3 \qquad (8)$$

$(PtO)_2$. The weak 550.9 cm^{-1} band shifts to 520.8 cm^{-1} with $^{18}O_2$ a slightly higher ratio than diatomic PtO. The mixed $^{16}O_2 + {}^{18}O_2$ experiment shows one dioxygen molecule, and the scrambled sample indicates two equivalent oxygen atoms are involved. This absorption is appropriate for a slightly nonplanar $(PtO)_2$ species made by reaction of a second Pt atom with the $Pt(O_2)$ complex:

$$Pt(O_2) + Pt \rightarrow (PtO)_2 \qquad (9)$$

$(O_2)PtO$. The band at 1174.2 cm^{-1} in the $^{16}O_2$ experiment, which increased slightly on high-temperature (25, 30, and 35 K) annealing is assigned to the O−O stretching mode of the $(O_2)PtO$ complex. The 1.0592 isotopic frequency ratio is consistent with an O−O stretching motion, and the 1:2:1 triplet pattern is evidence of *two equivalent* oxygen atoms. The appearance of this band following annealing is a common pattern for dioxygen complexes, which typically form as a result of O_2 diffusion in the argon matrix. Finally, it is important to note that this set of bands was not observed by previous investigators whose methodology did not form the necessary PtO reagent molecule. The position of this band, which is red-shifted 378 cm^{-1} from that of molecular oxygen (1552 cm^{-1} in argon),[34] indicates substantial weakening of the O−O bond and is typical of side-bound dioxygen complexes. It is clear, however, that the PtO oxide interacts less strongly with O_2 than does the platinum atom in $Pt(O_2)$.

OOPtO. The 1.0593 isotopic frequency ratio of the band at 1402.1 cm^{-1} is also consistent with an O−O stretching motion. However, the quartet pattern exhibited by this band with the isotopically scrambled precursor is indicative of a molecule with *two inequivalent* oxygen atoms and is assigned here to the O−O stretch of the OOPtO complex. This band grew substantially on higher temperature annealing (Figure 2), even more than the 1174.2 cm^{-1} band of $(O_2)PtO$, despite the lower calculated energy for $(O_2)PtO$. Unfortunately, no lower frequency Pt−O stretching mode was observed for either O_2 complex with PtO. As was the case for $(O_2)PtO$ above, the bond weakening effect on O_2 is expected to be substantially less for PtO than for a platinum atom alone. This is borne out by the B3LYP frequency calculations of PtOO and OOPtO, although these calculations seem to overestimate this effect somewhat even for OOPtO. Also, as was the case for $(O_2)PtO$, the bands reported here were not observed in previous experiments, which lacked the PtO precursor necessary for the formation of OOPtO.

The lack of a shift from the pure isotopic bands in the $^{16}O_2 + {}^{18}O_2$ experiments shows that there is no measurable coupling between the O−OPtO and OOPt−O stretching modes. The growth of weak intermediate bands with $^{16}O_2 + {}^{18}O_2$ suggests that some OOPtO is produced from the O + OPtO reaction on annealing.

Nickel counterparts were observed for both of these dioxygen platinum oxide complexes, namely, OONiO and $(O_2)NiO$ at 1393.7 and 1095.5 cm^{-1}, respectively, but no evidence was found for NiO_3.[30] Apparently, the larger Pt atom is required for the VI oxidation state. The spectra were searched for a possible O_2 complex with OPtO like that formed with ONiO and readily with OIrO,[30,31] and no reasonable candidates were found.

Conclusions

The reaction of laser-ablated platinum atoms with dioxygen yielded the platinum complexes $Pt(O_2)$ and $(O_2)Pt(O_2)$ observed previously with thermal atoms, and the platinum oxides PtO, OPtO, and PdO_3 not observed previously, and the oxide complexes $(O_2)PtO$ and OOPtO, while similar reactions with palladium yielded only the $Pd(O_2)$ and $(O_2)Pd(O_2)$ complexes. These products were isolated in argon matrices, studied by infrared spectroscopy, and identified by isotopic frequency shifts and correlation with B3LYP frequency calculations.

Of particular note is the lack of any significant products other than dioxygen complexes in the palladium experiments. It was expected that the high kinetic energy imparted to palladium atoms by laser ablation would be adequate to overcome the activation energy to the formation of PdO and OPdO. Even in the presence of O atoms and O_3, PdO is apparently not formed. Analogous molecules were observed in previous experiments for nickel[30] and here with platinum, but not with palladium. This is attributed to the unusually stable (d^{10}) configuration of ground-state palladium.

In the platinum experiments, the linear OPtO molecule is formed on deposition by insertion of energetic Pt atoms into dioxygen and by photolysis of $Pt(O_2)$. Clearly, the side-bound complex can be activated to give the dioxide. This result is an interesting complement to the previous observations of an oxygen complex on solid platinum as characterized by an 860

cm^{-1} fundamental[1] and the cleavage of O_2 on platinum surfaces.[7−9] In this regard, Manceron has recently demonstrated that Ni(O_2) rearranges to ONiO on photolysis.[31] The stable linear platinum dioxide molecule is analogous to ONiO and to OCoO, ORhO, and OIrO from the previous transition metal family.[30,32,35]

These platinum experiments, employing laser-ablated metal atoms, have also produced the PtO molecule, which was not observed in earlier thermal experiments;[10] this observation further attests the need for excess energy in Pt atoms in order to form PtO and O atoms. In the presence of O atoms a possible Pt(VI) oxide PtO_3 may be formed. Finally, the PtO molecule associated further upon annealing to give the new OOPtO and (O_2)PtO complexes, which suggests catalytic activity for the oxide as well.

Acknowledgment. We thank the National Science Foundation (CHE 97-00116) for financial support.

References and Notes

(1) Avery, N. R. *Chem. Phys. Lett*. **1983**, *96*, 371.
(2) Morrow, B. A.; McFarlane, R. A.; Moran, L. E. *J. Phys. Chem.* **1985**, *89*, 77.
(3) Weber, M F.; Digman, M. J.; Park, S. M. *J. Electrochem. Soc.* **1986**, *133*, 734.
(4) Zinola, C. F.; Castro-Luna, A. M.; Tricia, W. E. *J. Appl. Electrochem.* **1994**, *24*, 119.
(5) Zinola, C. F.; Castro-Luna, A. M.; Tricia, W. E. *J. Appl. Electrochem.* **1994**, *24*, 531.
(6) Wartnaby, C. E.; Stuck, A.; Yeo, Y. Y. *J. Phys. Chem.* **1996**, *100*, 12483.
(7) Zambelli, T.; Barth, J. V.; Wintterlin, J. *Nature* **1997**, *390*, 495.
(8) Novakova, J.; Brabec, L. *J. Catal.* **1997**, *166*, 186.
(9) Chen, W.; Lu, H.; Prader, C.-M. *J. Catal.* **1997**, *172*, 3.
(10) Huber, H.; Klozbücher, W.; Ozin, G. A.; Vander Voet, A. *Can. J. Chem*. **1973**, *51*, 2722.
(11) Nilsson, C.; Scullman, R.; Mehendale, N. *J. Mol. Spectrosc*. **1970**, *35*, 172. Scullman, R.; Sassenberg, U.; Nilsson, C. *Can. J. Phys.* **1975**, *53*, 1991. Jansson, K.; Scullman, R. *J. Mol. Spectrosc.* **1976**, *61*, 299. Sassenberg, U.; Scullman, R. *J. Mol. Spcetrosc.* **1977**, *68*, 331.
(12) Sassenberg, U.; Scullman, R. *Phys. Ser*. **1983**, *28*, 139. See also the following. Srdanov, V. I.; Harris, D. O. *J. Chem. Phys.* **1987**, *89*, 2748.
(13) Frum, C. I.; Engleman, R., Jr.; Bernath, P. F. *J. Mol. Spectrosc*. **1991**, *150*, 566.
(14) Steimle, T. C.; Jung, K. Y.; Li, B.-Z. *J. Chem. Phys.* **1995**, *103*, 1767.
(15) Williams, C. T.; Tolia, A. A.; Chan, H. Y. H.; Takoudis, C. G.; Weaver, M. J. *J. Catal*. **1996**, *163*, 63.
(16) Burkholder, T. R.; Andrews, L. *J. Chem. Phys.* **1991**, *95*, 8697. Hassanzadeh, P.; Andrews, L. *J. Phys. Chem.* **1992**, *96*, 9177.
(17) Frisch, M. J.; Trucks, G. W.; Schlegel, H. B.; Gill, P. M. W.; Johnson, B. G.; Robb, M. A.; Cheeseman, J. R.; Keith, T.; Petersson, G. A.; Montgomery, J. A.; Raghavachari, K.; Al-Laham, M. A.; Zakrzewski, V. G.; Ortiz, J. V.; Foresman, J. B.; Cioslowski, J.; Stefanov, B. B.; Nanayakkara, A.; Challacombe, M.; Peng, C. Y.; Ayala, P. Y.; Chen, W.; Wong, M. W.; Andres, J. L.; Replogle, E. S.; Gomperts, R.; Martin, R. L.; Fox, D. J.; Binkley, J. S.; Defrees, D. J.; Baker, J.; Stewart, J. P.; Head-Gordon, M.; Gonzalez, C.; Pople, J. A. *Gaussian 94*, revision B.1; Gaussian, Inc.: Pittsburgh, PA, 1995.
(18) Lee, C.; Yang, E.; Parr, R. G. *Phys. Rev. B* **1988**, *37*, 785.
(19) Dunning, T. R., Jr.; Hay, P. J. In *Modern Theoretical Chemistry*; Schaefer, H. F., III, Ed.; Plenum: New York, 1976.
(20) Hay, P. J.; Wadt, W. R. *J. Chem. Phys.* **1985**, *82*, 299.
(21) Kirchner, E. J. J.; Baerends, E. J.; van Slooten, U.; Kleyn, A. W. *J. Chem. Phys.* **1992**, *97*, 3821.
(22) Chung, S.-C.; Krüger, S.; Pacchiori, G.; Rösch, N. *J. Chem. Phys.* **1995**, *102*, 3695.
(23) Andrews, L.; Spiker, R. C., Jr. *J. Phys. Chem.* **1972**, *76*, 3208.
(24) Chertihin, G. V.; Saffel, W.; Yustein, J. T.; Andrews, L.; Neurock, M.; Ricca, A.; Bauschlicher, C. W., Jr. *J. Phys. Chem*. **1996**, *100*, 5261.
(25) Chertihin, G. V.; Andrews, L. *J. Chem. Phys.* **1998**, *108*, 6404.
(26) Zhou, M. F.; Hacaloglu, J.; Andrews, L. *J. Chem. Phys.* **1999**, *110*, 9450.
(27) Smith, D. W.; Andrews, L. *J. Chem. Phys.* **1972**, *60*, 81.
(28) Bytheway, I.; Wong, M. W. *Chem. Phys. Lett.* **1988**, *282*, 219.
(29) Raziunas, V.; Macur, G.; Katz, S. *J. Chem. Phys.* **1965**, *43*, 1010. See p 1015.
(30) Citra, A.; Chertihin, G. V.; Andrews, L.; Neurock, M. *J. Phys. Chem. A* **1997**, *101*, 3109.
(31) Manceron, L. Unpublished results (Ni + O_2).
(32) Citra, A.; Andrews, L. *J. Phys. Chem. A* **1999**, *103*, 4182.
(33) Darling, J. H.; Ogden, J. S. *J. Chem. Soc., Dalton Trans.* **1972**, 2496.
(34) Andrews, L.; Smardzewski, R. R. *J. Chem. Phys.* **1973**, *58*, 2258.
(35) Chertihin, G. V.; Citra, A. C.; Andrews, L.; Bauschlicher, C. W., Jr. *J. Phys. Chem. A* **1997**, *101*, 8793.